Vol 16 No 4, April 2007
1009-1963/2007/16(04)/1077-07

Chinese Physics

© 2007 Chin. Phys. Soc.
and IOP Publishing Ltd

Open loop control of vortex-induced vibration of a circular cylinder*

Chen Zhi-Hua(陈志华)†, Fan Bao-Chun(范宝春), Zhou Ben-Mou(周本谋), and Li Hong-Zhi(李鸿志)

Key Lab of Transient Physics, Nanjing University of Science & Technology, Nanjing 210094, *China*

(Received 24 November 2005; revised manuscript received 23 July 2006)

In this paper both numerical and experimental investigations have been carried out to suppress the vortex-induced vibration (VIV) of a circular cylinder in an electrically low-conducting fluid. The electromagnetic forces (Lorentz forces) in the azimuthal direction were generated through the mounted electrodes and magnets locally on the surface of the cylinder, which have been proved having an accelerating effect to the fluid on the surface of the cylinder. Results of computations are presented for synchronous vibration phenomenon of a cylinder at $Re = 200$, which are in good agreement with previous computational results. With the Lorentz forces loaded, the VIV of the cylinder has been suppressed successfully. Experimental results have also shown the same tendency and are in reasonable agreement with the numerical results.

Keywords: vortex-induced vibration, open-loop control, flow control, Lorentz force
PACC: 4700, 4715C

1. Introduction

Vortex induced vibration (VIV) of a bluff body is very common in application and also a challenging area of fluid mechanics, which continues to present problems to engineering designers in the fields of aeronautics, off-shore engineering, civil, chemical and mechanical engineering. Ever since the beginning of the last decade, the widespread occurrence of fluid/structure interaction problems has drawn the attention of researchers in finding ways to predict, weaken or even suppress this self-excited vibration. Over the last few decades, much experimental and numerical works have been performed on these fluid–structure vibration problems including forced vibration and free vibration of a cylinder. In the present effort, only self-excited vibration problems will be discussed.

Representative experimental investigations of VIV of a cylinder have established some important conclusions.[1,2] For instance, VIV is a self-limiting process with an upper bound for the amplitude of the vibrations; the magnitude of the lift force depends on the vibration amplitude, which itself has some relation with the reduced damping and the phase difference between the lift force and the motion of the cylinder. Recently, using a laser vibrometer and a laser Doppler anemometer, So *et al*[3] measured the synchronization phenomenon of a freely vibrating cylinder. Their results showed that cylinder vibrations have little or no effect on the mean drag and the normalized mean field. Bearman and Brankovic[4] measured the VIV of a plain circular cylinder and cylinder fitted with strakes and bumps. Experiments performed in water with mass ratio in a range from about 1.5 to 5.5 and combined mass and damping values between 0.002 and 0.007. They found that the amplitudes of vibration for cylinders with strakes or bumps were less than those for a plain cylinder. Recently, Pan *et al*[5] discussed the influence of axial vibration on free surface flows in an open cylindrical container.

Several different computational approaches have also been developed to calculate the flow field for this problem. Using the discrete vortex method incorporating the vortex-in-cell (VIC) method, Zhou *et al*[6] described the 2D VIV problem with vorticity-streamfunction equation at $Re = 200$. Their results showed that fluid damping is responsible for a limit-cycle oscillation behaviour and the cylinder oscillations could be as large as 0.57 diameter of the

*Project supported by the Scientific Research and Development Foundation of Nanjing University of Science and Technology, China (Grant No XKF05070) and Scientific Research Foundation for the Returned Overseas Chinese Scholars, State Education Ministry, China.
†E-mail: zhchen@mail.njust.edu.cn

cylinder under certain flow conditions and structural properties. Willden and Graham [7] used a first-order simulation to solve the 2D incompressible Navier–Stokes (N-S) equations in velocity–vorticity formulation, the Poisson equation relating pressure to velocity is solved by using the finite element method. Their presented numerical results for flow-induced transverse vibrations of a rigid two-dimensional low mass cylinder, elastically mounted with zero damping at a low Reynolds number $(50-320)$, and the oscillatory frequency was found to be controlled by the fluid via its added mass. Al-Jamal and Dalton[8] performed a 2D LES calculation of a freely vibration of cylinder wake at a Reynolds number of 8000. In spite of the shortcomings of a 2D representation, their results showed the expected vibratory response of the cylinder and are consistent with experimental values, and a beating behaviour in the oscillation was observed which diminished considerably as the damping value of cylinder was increased.

Investigations on the suppression of VIV have not been as extensive as VIV studies, and only a few theoretical control procedure and experimental methods have been developed,[9,10] moreover, it is still a long way for applying those theoretical control algorithms practically. On the other hand, passive and active VIV control methods developed experimentally have shown some applications background. For example, Owen *et al*[10] conducted some passive control experiments of VIV; they use a circular cross-sectional body with a sinuous axis and a circular cylinder with hemispherical bumps attached, their results have shown that the suppression of vortex shedding and drag reduction up to 47% within a wide range of Reynolds numbers. So far control of VIV is attracting more interest due to its applicable importance; our goal is to develop a method that can suppress the VIV efficiently and also can be applied practically.

Active control of cylinder wake with electromagnetic forces applied on the whole surface of the cylinder was first developed experimentally and numerically by Weier *et al*[11] latterly, localized Lorentz forces with location optimized was developed both experimentally and numerically.[12,13] In present investigation, the open loop control method, which used localized Lorentz force as the actuator, was developed for suppressing VIV of a freely vibrating cylinder. This work is an extension of our previous investigations. In this paper, VIV of a freely cylinder has been simulated two-dimensionally. The Lorentz force which was taken as the open loop control actuator, is applied for suppressing vortex induced vibration problems. Furthermore, to confirm our computational results, experiments have also been carried out for both VIV of a circular cylinder and its suppression with electrodes and magnets covered along the span of the cylinder surface. Both our computational and experimental results show that the VIV of a cylinder can be suppressed successfully at low and moderate Reynolds number with the use of localized Lorentz forces as the actuator

2. Numerical analysis

For solving such fluid–structure problems, a general technique called the arbitrary Lagrangian–Euler (ALE) method in conjunction with spectral discretization on unstructured grids is used. An alternative and simple approach is to attach the coordinate system to the body and solve the N-S equations in a moving frame of reference.[5,14] In an electrically conducting fluid, the two-dimensional incompressible N-S equations can be written as

$$\frac{\partial \boldsymbol{V}}{\partial t} + (\boldsymbol{V}\cdot\nabla)\boldsymbol{V} = -\nabla p + \frac{2}{Re}\nabla^2\boldsymbol{V} + N\boldsymbol{F}, \tag{1}$$

$$\nabla\cdot\boldsymbol{V} = 0\,. \tag{2}$$

Re is Reynolds number, where $Re = 2u_\infty a/\nu$. u_∞, a, ν denote the free-stream velocity far from the cylinder, the cylinder radius and the kinematic viscosity respectively. $N = j_0 B_0 a/\rho u_\infty^2$, denotes the interaction parameter. $\boldsymbol{F}$ is the dimensionless Lorentz force which is defined as $\boldsymbol{F} = \boldsymbol{J}\times\boldsymbol{B}$, where $\boldsymbol{B}$ and $\boldsymbol{J}$ denote the magnetic induction intensity and current density respectively. In low conducting fluids like seawater, etc., the induced electrical current by magnetic field is too small compared to the current associated with the electric field, and is thus neglected, thus we have $\boldsymbol{J} = \sigma\boldsymbol{E}$, where σ is the electric conductivity, and $\boldsymbol{E}$ refers to the electric field intensity.

Transforming the above N-S equations into the polar coordinate system, and introducing the exponential-polar coordinates system (ξ,η), $r = \mathrm{e}^{2\pi\xi}$, $\theta = 2\pi\eta$, after defining the stream function ψ and vorticity Ω as

$$\frac{\partial\psi}{\partial\eta} = U_r = H^{1/2}(u_r + \overline{u}_r),$$

$$-\frac{\partial\psi}{\partial\xi} = U_\theta = H^{1/2}(u_\theta + \overline{u}_\theta),$$

$$\Omega = \frac{1}{r}\frac{\partial(ru_\theta)}{\partial r} - \frac{1}{r}\frac{\partial u_r}{\partial\theta},$$

where u_r and u_θ is the projection of the velocity $\boldsymbol{V}$ in the direction of r, θ respectively, and $H = 4\pi^2 \mathrm{e}^{4\pi\xi}$, then we can obtain the vorticity–streamfunction formulation of the N-S equations in the transformed system of coordinates as

$$H\frac{\partial \Omega}{\partial t} + \frac{\partial (U_r \Omega)}{\partial \xi} + \frac{\partial (U_\theta \Omega)}{\partial \eta} = \frac{2}{R_e}\Big(\frac{\partial^2 \Omega}{\partial \xi^2} + \frac{\partial^2 \Omega}{\partial \eta^2}\Big) + NH^{\frac{1}{2}}\Big(\frac{\partial F_\theta}{\partial \xi} + 2\pi F_\theta\Big), \quad (3)$$

$$\frac{\partial^2 \psi}{\partial \xi^2} + \frac{\partial^2 \psi}{\partial \eta^2} = -H\Omega. \quad (4)$$

Assume that the cylinder vibration is permitted only transverse to the freestream direction (y), and take the cylinder diameter d and free-stream velocity u_∞ as the characteristic length and velocity scales respectively, thus, coupled cylinder vibration equation can be described in its one-degree of freedom form as

$$\frac{\mathrm{d}^2 Y}{\mathrm{d}t^2} + \frac{4\pi\alpha}{U_{\mathrm{re}}}\frac{\mathrm{d}Y}{\mathrm{d}t} + \Big(\frac{2\pi}{U_{\mathrm{re}}}\Big)^2 Y = \frac{C_{\mathrm{l}}}{2M}, \quad (5)$$

where Y denotes the dimensionless displacement of the cylinder in the y direction instantaneously, and U_{re} is the reduced velocity defined as $U_{\mathrm{re}} = u_\infty / f_{\mathrm{n}}$, where f_{n} is the natural frequency of the cylinder. M is the mass ratio, $M = m/\rho d^2$, m is the cylinder mass per unit length, ρ refers to the flow density, C_{l} denotes the lift force coefficient, $C_{\mathrm{l}} = F_{\mathrm{ty}}/(\rho u_\infty^2 d/2)$, and the total lift force F_{ty} is the projection of total drag in the y direction, while the total drag is calculated by integrating the pressure and shear stress along the cylinder body surface.

This coupled fluid–cylinder problem is solved by the following strategy. At each time step, the vorticity-streamfunction and vibration equations are solved independently to decouple their solutions. While the vorticity-streamfunction equations are solved, the aerodynamic lift force acting on the cylinder can be obtained. The lift force is then an input to the vibration solver which predicts the position of the cylinder vibration and velocity of the cylinder responding to the fluctuation of lift force. Once the position of the cylinder is determined, this new cylinder position and velocity will be used as updated boundary conditions for next time level calculation. The flow is considered two-dimensional flow at infinity. The impulsive start is simulated by using potential flow as initial condition except on the surface of the cylinder where the absence of slip boundary condition applied.

The vorticity transport equation (3) is solved firstly with the use of Alternative-Direction Implicit algorithm, and the accuracy of the numerical scheme is second order in space and first order in time. Streamfunction equation (4) is a Poisson equation which can be integrated by means of a fast Fourier transform algorithm. Detailed descriptions can be found in Ref.[13]. Lastly, the vibration equation is solved by using the three-order Runge–Kutta method, which can be easily found in the literature.

3. Numerical results and discussion

Numerical results for all of our simulations are chosen at Reynolds number $Re = 200$ with the computational step $\Delta\xi = 0.004$, $\eta = 0.002$ and $\Delta t = 0.005$. The cylinder is assumed to vibrate freely only in the cross-flow direction and the mass ratio is chosen to be equal to 1.

3.1. Vortex induced vibration of a cylinder

In a structure damper system, when the forcing frequency is close to the damped natural frequency, the structure oscillates at the forcing frequency and the maximum response amplitude known as resonance (or synchronization) occurs. To obtain a significant VIV response in our simulation, we tune the natural frequency of the cylinder vibration close to the frequency of the vortex shedding. The fixed-cylinder vortex shedding frequency can be used to estimate this. Based on our computational results, the Strouhal number corresponding to the dominant frequency of the lift variation is 0.183. The Strouhal number is defined as $S_t = f_{\mathrm{d}}/u_\infty$, where f is the vortex shedding frequency evaluated from simulation.

The cylinder was assumed initially free to vibrate in the transverse direction and a self-limiting process with an upper bound for the vibration amplitude with respect to the mass damping parameter was also observed. Table 1 shows that the overall agreement with the calculated data obtained in our simulations is comparable to that in Refs.[15 – 20]. In Table 1, for a VIV of a circular cylinder at $Re = 200$, many simulation methods have been developed such as finite volume method,[15] finite difference method,[16] vortex method[6,18] and finite element method,[17,19,20] which

give a value of average $C_{\rm d}$ ranging from 1.17 to 1.476 and S_t varies from 0.162 to 0.20. In addition, $C_{\rm l}'$ in Table 1 is the root mean square (rms) value of lift coefficient which varies from 0.219 to 0.54. The obtained present results are slightly higher than the average value of theirs and within a reasonable area.

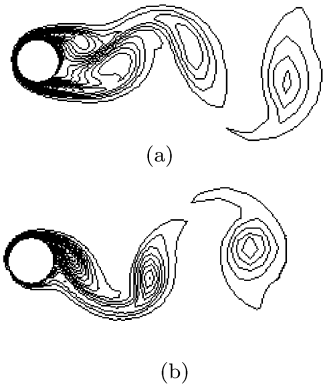


Fig.1. Typical vortex pattern of our computational results for a circular cylinder at $Re = 200$. (a) A stationary cylinder; (b) VIV of a free cylinder.

Figure 1 displays the comparison of our calculated vortex pattern of a stationary cylinder and a VIV of free vibration, which are also comparable to those of our experimental results (Figs.7(a) and 7(b)). Changes of vortex pattern of the cylinder during vibration can be seen in Fig.2 at almost one cycle.

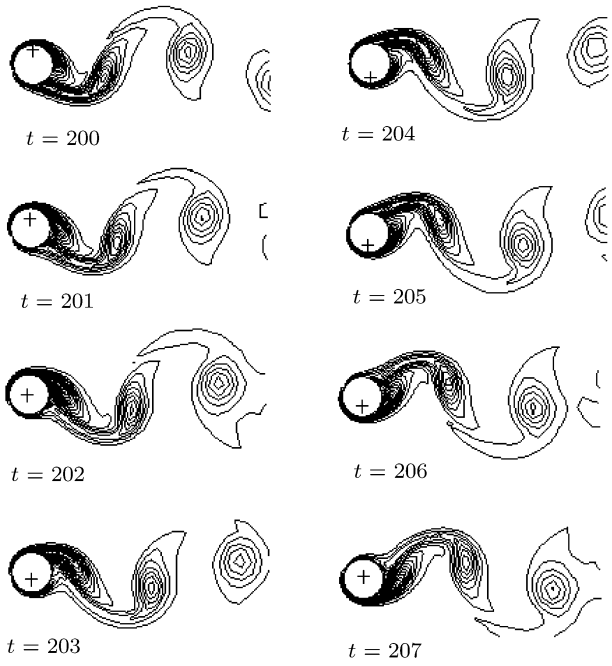


Fig.2. Vortex pattern of a vibrating cylinder at different position. The cross (+) corresponds to the initial location of the cylinder centre.

Table 1. Comparison of our results with other calculated results.

	$\bar{C}_{\rm d}$	$C_{\rm l}'$	S_t
Finite volume method (Braza *et al*[15], 1986)	1.35	0.54	0.2
Upwind difference scheme (Rogers *et al*[16], 1990)	1.29	0.46	0.185
Finite-element method (Li *et al*[17], 1991)	1.17	0.35	0.180
Random vortex method (Stansby and Slaouti[18], 1993)	1.317	0.248	0.166
Vortex-in-cell method (Zhou *et al*[6] 1999)	1.476	0.219	0.162
Finite element method (Meneghini *et al*[19] 2001)	1.30	0.47	0.196
Finite element method (So *et al*[20], 2003)	1.333	0.431	0.180
Average of all above	1.319	0.388	0.181
Present results	1.345	0.44	0.183

3.2. Suppression of VIV of a cylinder

When localized Lorentz forces are used, their precise location is critical in the effectiveness of suppressing flow separation. It is known that if the actuator is located too far from the separation point on the surface of the cylinder, suppression could not be obtained. Since the uncontrolled flow is at $Re = 200$, the separation point on the cylinder is at about $\pm 110^\circ$ from the front stagnation point. We have selected the location of our actuators slightly upstream of the separation point, which is at $95^\circ \leq |\theta| \leq 175^\circ$ from the stagnation point, and successfully suppressed the vortex shedding of a stationary cylinder. However, for a freely vibrating cylinder, we found that the active area of the Lorentz force should be extended, which was chosen at $90^\circ \leq |\theta| \leq 175^\circ$ from the stagnation point. The interaction parameter N for the control was chosen to $N = 2.5$ in our computation. The control is applied at time $t = 300$ when the flow is in its well-developed VIV region. Time evolution of vortex

patterns for the same flow after the open loop control applied was shown in Fig.3. Time history of the drag, lift coefficients and vibration amplitude of the cylinder for the open loop control are shown in Figs.4 and 5 respectively.

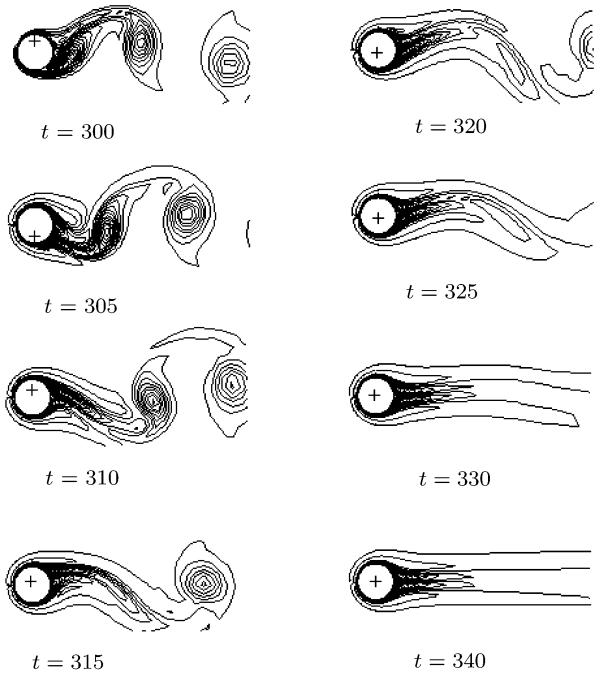


Fig.3. Instantaneous vortex pattern showing the suppression of the VIV. The Lorentz force is applied at time $t = 300$ and successive times. The cross (+) corresponds to the initial location of the cylinder centre.

It is evident that our open loop control method has modified the flow significantly. When there is no Lorentz force loaded, the flow is unsteady and shows the characteristic features of the Von Karman vortex street (Fig.2). When the Lorentz force is applied, no more large vortices appear except tat the last pair of vortices shed away from the cylinder and the flow separation region is diminished greatly; at the same time, the amplitude is also suppressed largely (Fig.5). After a period of time, the vibration of cylinder suppressed fully and oscillations downstream vanished finally. The vorticity lines behind the cylinder become flat, straight and horizontal. The whole flow becomes almost symmetric with respect to the centreline (Fig.3, $t = 340$).

The time history of the force coefficient and amplitude of cylinder also show that the suppressive effect of open loop control turned on. Before the control, the lift oscillates with a frequency of about 0.092 which is the same as the vibration frequency of the cylinder, and the drag force frequency is double of that. After the control, all their oscillations become weak, and finally disappear fully (Figs.4 and 5).

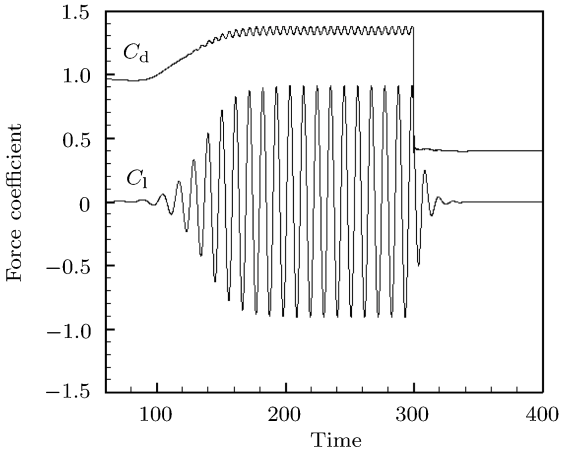


Fig.4. Time history of the drag and lift force coefficients.

Based on our simulation, by using open loop control method, to fully suppress the VIV of a cylinder will cost more time and energy than that of vortex shedding in comparison with Ref.[13], which also means that it is more difficult for controlling VIV problems than for the vortex shedding of a stationary body.

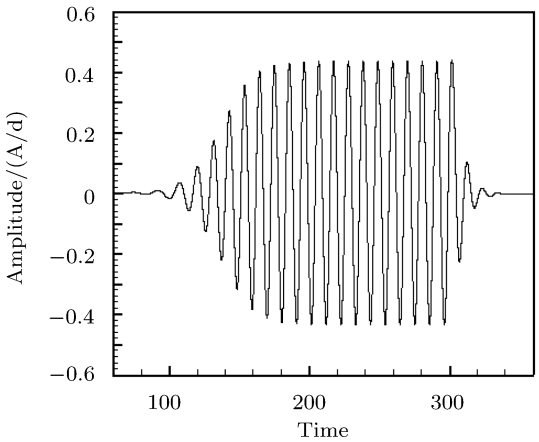


Fig.5. Displacement of the free cylinder before and after open control is applied.

4. Experimental approaches

Experiments were performed in the mixture of copper sulphate ($CuSO_4$) and water which has almost the same density and conductivity of seawater. The colour of the solution is blue, so a marker in which is required to be dissolved. Furthermore, the matched density of the solution needs to be chosen for flow

visualization, in our experiments, Potassium permanganate (KMnO4) was selected which gives a dark violet marker. A schematic image is shown in Fig.6.

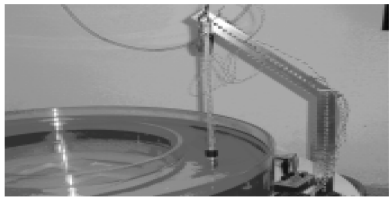
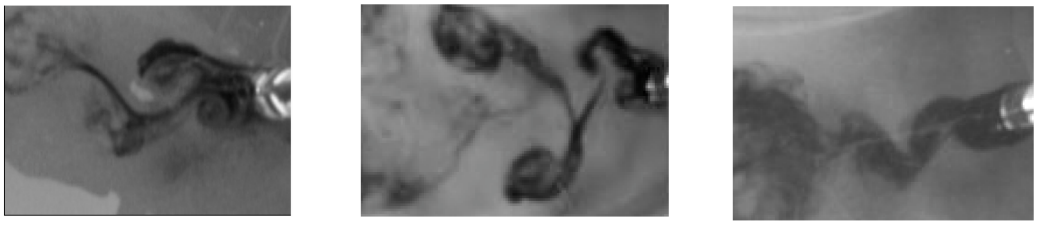


Fig.6. Schematic image of the experimental set-up

To achieve low damping of the cylinder, a long metal sheet was used to mount the cylinder working as a pendulum and the length of the pendulum can be adjusted to make the synchronization phenomenon occur. The vibration of the attached cylinder is transverse of the flow and predominantly in the horizontal plane. At the top end of the sheet metal, a strain gage sensor was installed for showing the vibrating amplitude. The magnitude of the exporting signal is proportional to the cylinder amplitude. The circular cylinder was covered with electrodes and magnets N, +, S, −, etc. along the span of the cylinder whose role was to create a Lorentz force symmetric with respect to the flow centreline and parallel to the body surface. Details of relative facilities and experimental techniques used in our experiments can be found in our published correlative references.



(a) (b) (c)

Fig.7. Visualized images illustrating the differences of vortex formation among (a) a stationary cylinder; (b) VIV of a cylinder; (c) Suppression of VIV with Lorentz force.

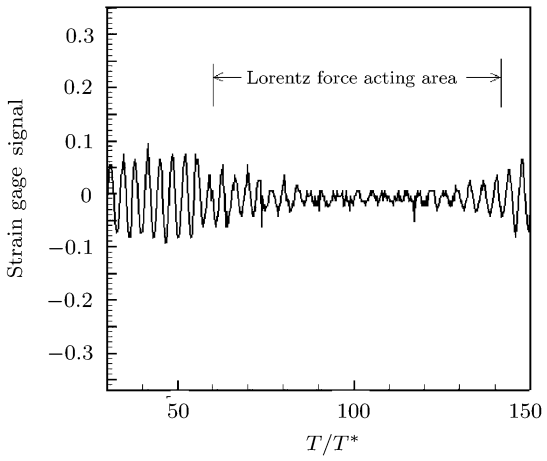


Fig.8. Signal of strain gage sensor showing the suppression of VIV.

Flow visualization of the vortex pattern for different conditions, (a) a stationary cylinder, (b) VIV of a cylinder and (c) suppression with Lorentz force were taken and displayed at Reynolds number of almost 1200. For a stationary cylinder (Fig.7(a)) the shear layers and the vortex roll-up are clearly visualized as well as a Von Karman vortex street behind the cylinder. However, when the cylinder is in synchronized motion (Fig.7(b)), the vortex pattern is similar to the classical wake pattern behind the stationary cylinder but the vortices will be a little far to the wake axis as they propagate downstream. When the actuators (Lorentz forces) on the cylinder surface were triggered (Fig.7(c)), just like our computational results, no more large vortices appear, and the vortex behind the cylinder shows weaker strength than the other two cases. Figure 8 shows the typical time histories of strain gage signal during suppression. It is clear that a drastic change occurs after the Lorentz force is added, the amplitude drops from a maximum of 0.07 in the absence of the Lorentz force to about 0.012 after being acted, about 83% attenuation. Furthermore, the signal after the addition of Lorentz force is significantly less periodical than free vibration. It is clear that the Lorentz force has a suppression effect to VIV.

5. Conclusions

VIV of a circular cylinder has been investigated at the Reynolds number of $Re = 200$. The transformation coordinates has been attached to the cylinder, which allows us to solve this fluid/structure problem in a loosely coupled algorithm. The calculated results can be comparable to other existing numerical results. Numerical computation has also performed with Lorentz force acted locally on the rear surface of the cylinder in an electrical low-conducting fluid. Furthermore, experiments were also carried out to investigate the suppression effect of the Lorentz force in the mixture of copper sulphate ($CuSO_4$) and water, which was trying to maintain almost the same conditions as those of numerical investigation. Both our numerical and experimental results for open loop control of VIV of a cylinder show that even with the Lorentz force generated locally with the separation point included on the surface of the cylinder, VIV of the circular cylinder can be suppressed successfully.

References

[1] Feng C C 1968 *M.A.Sc. thesis, University of British Columbia* (Canada: Vancouver B C)

[2] Griffin O M and Koopmann G H 1977 *Journal of Sound and Vibration* **54** 435

[3] So R M C, Zhou Y and Liu M H 2000 *Experiments in Fluids* **29** 130

[4] Bearman P and Brankovic M 2004 *European Journal of Mechanics B/Fluids* **23** 9

[5] Pan X and Jin W 2005 *Chin. Phys.* **14** 422

[6] Zhou C Y, So R M C and Lam K 1999 *Journal of Fluids and Structures* **13** 65

[7] Willden R H J and Graham J M R 2001 *Journal of Fluids and Structure* **15** 659

[8] Al-Jamal H and Dalton C 2004 *Journal of Fluids and Structures* **19** 73

[9] Gattulli V and Ghanem R 1999 *International Journal of Non-Linear Mechanics* **34** 853

[10] Owen J C, Bearman P W and Szewczyk A A 2001 *Journal of Fluids and Structures* **15** 597

[11] Weier T, Gerbeth G, Mutschke G and Platacis G 1998 *Exp. Therm. Fluid Sci.* **16** 84

[12] Chen Z H 2001 *Ph.D dissertation New Jersey Institute of Technology* (USA: New Jersey)

[13] Chen Z H and Fan B 2002 *Acta Mechanica Sinica* **34** 978 (in Chinese)

[14] Lu X Y and Dalton C 1996 *Journal of Fluids and Structures* **10** 527

[15] Braza M, Chassaing P H and Minh H 1986 *J. Fluid Mech.* **165** 79

[16] Rogers S E and Kwak D 1990 *AIAA Journal* **28** 253

[17] Li J, Chambarel A, Donneaud M and Martin R 1991 *Computers and Fluids* **19** 155

[18] Stansby P K and Slaouti A 1993 *International Journal for Numerical Methods in Fluids* **17** 1003

[19] Meneghini J R, Saltara F, Siqueira, C L R and Ferrari J A 2001 *Journal of Fluids and Structures* **15** 327

[20] So R M C, Liu Y and Lai Y G. 2003 *Journal of Fluids and Structures* **18** 287